

1 **Complex multi-source emissions quantification results for the PoMELO**
2 **vehicle measurement system, test results from the CSU METEC facility**

3
4 Thomas E. Barchyn^{*,1}, Chris H. Hugenholtz¹

5
6 ¹Department of Geography, University of Calgary, 2500 University Drive NW, T2N 1N4, Calgary,
7 Alberta, Canada

8
9 *email: tbarchyn@ucalgary.ca, twitter: @tbarchyn

10
11 **This manuscript is a non-peer reviewed preprint submitted to EarthArXiv**

12

13 **1. Abstract**

14 Methane emissions from oil and gas sites are often characterized by mixed plumes from multiple sources
15 in close proximity. This presents a challenge for screening methods that rely on emissions quantification to
16 direct and prioritize follow-up inspections. Here, we present results from experiments evaluating mixed-
17 source quantifications using the University of Calgary Portable Methane Leak Observatory (PoMELO)
18 conducted at the Colorado State University Methane Emissions Technology Evaluation Center (CSU
19 METEC). PoMELO is a vehicle-based screening system that is designed for operator-led surveys of
20 methane emissions at upstream oil and gas sites, producing detections, localizations, and emissions
21 quantifications while on site. Mock upstream pads were configured with 1-6 emissions points and the
22 PoMELO system was used to quantify emissions rates at the equipment scale for each piece of equipment.
23 Over 5 days of testing in a wide diversity of conditions, 88 individual experiment pads were surveyed at
24 the equipment scale, with 1-6 emitting equipment per survey (total surveyed equipment = 209). The
25 uncalibrated model was effective at measuring differences in rates: compared against real releases there
26 was a linear calibration factor of 6.77 ($r^2 = 0.71$). Results were more accurate in conditions with stable flow.
27 Experiments with measurements further downwind were more accurate, and results improved when
28 considering pooled data on each pad (linear model fit $r^2 = 0.84$), reflecting errors in the model attributable
29 to disambiguating methane in mixed plumes. Results suggest PoMELO has practical utility for
30 understanding upstream methane emissions at the equipment and total pad scale.

31 **2. Introduction**

32 In the upstream oil and gas industry, hundreds of thousands of wellpads are distributed across different
33 production areas. These pads typically contain one or several pieces of equipment such as wellheads,
34 separators, tanks, risers, and other production equipment. Methane emissions occur from equipment either
35 by design (e.g., vents and combustion emissions), or by accident (e.g., leaks) (see Alvarez et al., 2018).

36
37
38 Methane is a damaging greenhouse gas, and there is significant effort worldwide to decrease methane
39 emissions from the oil and gas industry (Ocko et al., 2021). However, methane emissions from upstream
40 sources are very poorly understood. Emissions from leaks are difficult to detect and can occur at any time
41 as equipment ages and fails. Emissions from sources such as vents that emit by design often vary through
42 time – or emit significantly more or less than the original design (e.g., Johnson et al., 2019; Zimmerle et
43 al., 2022).

44
45 Oil and gas producers face a considerable challenge managing their emissions and operating cost-effective
46 abatement programs without accurate emissions data. Collecting this data is costly as the scale of oil and
47 gas infrastructure is immense, with equipment distributed across huge geographies, often in remote
48 locations. This challenge has spurred considerable research and development. A wide diversity of
49 approaches for collecting data from upstream sites are presently in use (Fox et al., 2019b; Ravikumar et al.,
50 2019).

51
52 From a scientific perspective, measuring methane emissions is very difficult. Methane cannot be seen and
53 has no odor. With qualitative methods such as optical gas imaging (OGI), intuition is often not reliable for
54 estimating emissions rates (Zimmerle et al., 2022). Accurate rate measurement requires complex plume
55 modeling, specialized instrumentation, and careful understanding of airflow on upstream sites (Fox et al.,
56 2019a).

58 To help advance the science of emissions quantification, the University of Calgary has developed the
59 PoMELO system, a field truck mounted methane detection and quantification system that serves as a testbed
60 for research, development, and education (Figure 1, Barchyn and Hugenholtz, 2020a). The system uses
61 measurements of wind, position, and methane concentration to automatically detect, map, and quantify
62 emissions on upstream sites. Data are resolved at the equipment scale (~ meters). PoMELO uses 3
63 instruments: (i) high performance open path methane sensor, (ii) GNSS, and (iii) anemometer. A computer
64 fuses instrument data streams at 10 Hz and automatically maps the position of emissions sources on the
65 pad, as well as providing triage grade source quantifications for emissions sources.
66



67
68 **Figure 1:** the University of Calgary Portable Methane Leak Observatory (PoMELO) system at the
69 Colorado State University Methane Emissions Technology Evaluation Center (CSU METEC).
70

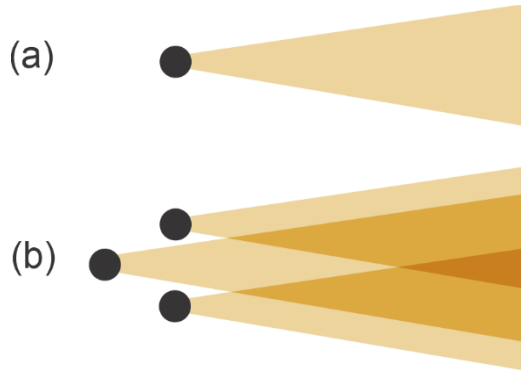
71 The most common work practice that is used with the PoMELO system is known as ‘OGI triage’, where
72 rapid detection and quantification with the PoMELO system is used to guide further emissions source
73 identification with an OGI camera (or similar close-range instrument) while on site. This work practice is
74 normally more efficient than traditional OGI surveys as using the PoMELO system to triage the equipment
75 that requires follow-up provides an opportunity for operators to immediately target surveys to certain parts
76 of a pad, and in cases omit OGI surveys in regions with no emissions or those below a target rate (see
77 further in Barchyn and Hugenholtz, 2020a).
78

79 The detection skill of the PoMELO system has been tested in a robust single-blind experiment (see Barchyn
80 and Hugenholtz, 2020a, 2020b). Results indicate the system had a minimum detection limit emissions rate
81 (90% probability of detection) below 0.0016 g/s (≈ 0.3 scfh, ≈ 0.2 m³ / day). The METEC test facility could
82 not meter rates low enough to produce a defensible probability of detection curve. This study was conducted
83 in a way such that the University of Calgary team reported results to METEC personnel before University
84 of Calgary were aware of release points, making the study blind.
85

86 Here, we focus on evaluating emissions quantification, using the same dataset as utilized in Barchyn and
87 Hugenholtz (2020a, 2020b). In particular, complex multi-source emissions configurations with close-range

88 mixed plumes were tested (see Figure 2). Multi-source emissions situations are realistic for many upstream
89 pads where leaks and vents are in close proximity. This differs from many controlled release experiments
90 where only a single release stack is used (e.g., Singh et al., 2021).

91
92



93 **Figure 2:** This report focuses on situations with overlapping plumes, where the methane from multiple
94 sources mix. Overlapping plumes are common on many upstream sites. In (a), the source (black dot)
95 produces one plume that is easily measured in isolation; however, in (b) multiple sources (black dots) each
96 have individual plumes that overlap, significantly increasing the complexity of plume modeling. The
97 multiple source configuration (b) is realistic for many upstream sites.

99

100 This study focuses on a new quantification engine for the PoMELO system. This model has not been
101 calibrated against empirical controlled release data and lacks a detailed assessment of system performance.
102 We use the following analysis steps to report information on the skill of the system:

103

- 104 (i) First, we compare the theoretical quantification engine results against complex multi-source
105 precision-controlled releases to understand the proportion of variance explained by the model
106 as a metric of uncalibrated skill. This helps to metric the triage performance of the model,
107 where the primary interest is finding the largest emissions sources.
- 108 (ii) Second, we use the release rates to develop a simple empirical correction. The dataset from
109 METEC is realistic and large, providing excellent data for a calibration.
- 110 (iii) Third, we evaluate condition dependence of the quantification engine to explore any
111 relationships between residuals and controlling conditions. This is useful to understand where
112 the model performs well, providing vital practical guidance for PoMELO users.

115

116 We then bring the results into context, comparing the results against similar studies and outline the
117 implications of these results for practical deployments of the PoMELO technology.

118

119 **3. PoMELO overview**

120 The PoMELO system is designed for producing data about emissions sources on upstream pads with one
121 visit, where all information necessary for emissions management is collected at one time. Modeling and
122 practical deployments have indicated this is an efficient approach to emissions management (Fox et al.,
123 2021). The system is designed to be easy to use to reduce training requirements and allow operators to
124 follow-up on detections and quantifications immediately, providing vital information while on the pad. The
125 general work practice is as follows:

126
127
128
129
130
131
132
133
134
135
136
137
138
139
140
141
142
143
144
145
146

- (i) **Rapid screen:** The PoMELO truck is driven around the site immediately upon arrival and a map of emissions locations is produced automatically as the system logs and integrates the data into a probability map of emissions locations. The operator takes note of emitting equipment, cross referencing the equipment types on the ground with detections and known emissions sources on the pad.
- (ii) **Equipment inventory:** With an inventory of emitting equipment, in cases augmented by OGI surveys or other close-range inspections, pieces of equipment are entered into the PoMELO system in preparation for quantification.
- (iii) **Quantification:** From this, the quantification engine automatically estimates the emissions rates associated with each piece of equipment onsite.
- (iv) **Component-scale surveys and investigation:** Armed with emissions rates and an accurate picture of where emissions are coming from on the site, the operators can conduct further investigation with close range technique like OGI, to precisely understand the source of emissions and determine the next course of action (e.g., repair, retrofit, further process analysis). The goal is to leave the site with a complete inventory of emissions sources and as much information as possible on the source to help abatement efforts.



147
148
149
150
151
152
153

Figure 3: The PoMELO system mounted on the roof of a standard field truck (after Barchyn and Hugenholtz, 2020a).

This study only evaluates the quantification performance of the system. We do not evaluate a full work practice with OGI follow-up. Metrics of OGI performance are documented elsewhere (see Zimmerle et al., 2020).

154
155
156
157
158
159
160
161
162
163
164
165
166
167
168
169
170
171
172
173
174
175
176
177
178
179
180
181

3.1. Quantification engine overview

The PoMELO system quantification engine is a close-range equipment-scale plume model. The model takes the following inputs:

Raw and assimilated measurement data: Data are measured automatically from the PoMELO system as it drives around a site. All sensor data are fused, corrected, and assembled in real-time and recorded as a timeseries. The system measures wind, methane concentration, temperature, pressure, vehicle orientation, velocity, and position. Additional diagnostic variables are included to help the system self-evaluate data quality.

Emitting equipment positions: In normal survey mode, emitting pieces of equipment are input by the user while on site. In this study we used the known emissions point locations provided by METEC staff.

From these input data, the algorithm produces individual emissions rates for each emitting piece of equipment. The model is specifically designed for close-range scenarios with many emissions points that create overlapped plumes. The quantification engine de-mixes the contributions from different sources and produces individual emissions rate estimates for each emitting piece of equipment.

4. Methods

4.1. METEC site overview

The METEC site was developed to examine the performance of technologies used to detect, localize, and quantify emissions. The site includes mock oil and gas pads with specially modified real oil and gas equipment that includes hidden leak locations (Figure 4, 5). There is no real oil and gas production on the site. Leak locations are a closely guarded secret. Further details about the site are discussed by Zimmerman et al. (2020).



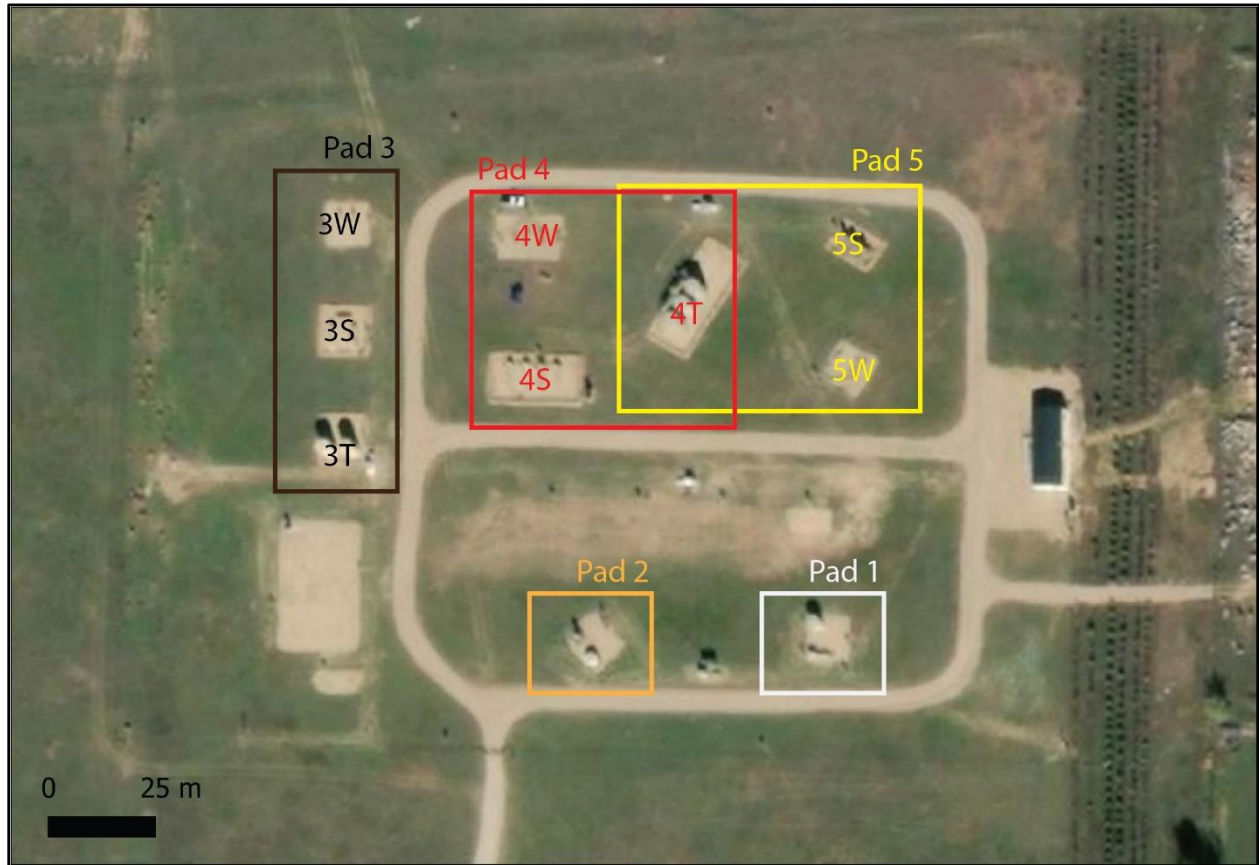
Figure 4: Mock equipment at the METEC site. The facility uses real production equipment that has been modified to have hidden leak points throughout. Participants do not know where the leaks are located, providing a robust environment to assess technology performance (after Barchyn and Hugenholtz, 2020a).

182
183
184
185
186
187
188
189
190
191
192
193
194
195

At METEC methane was sourced from high pressure natural gas (approximately 85% methane by mole fraction). The precise concentration mix was determined by gas chromatograph. While metered as a bulk flow, all emissions rates reported here are only reported in methane, in g/s.

Metering at METEC involves several steps. First, the high pressure gas was cut to lower pressures before running into a thermal mass flow meter. Next, the gas was run through a combination of 0-3 orifice plates to bring release rate(s) close to target rate(s). In experiments where multiple release points were supplied from the same flow meter, each release point was run in isolation to develop a calibrated flow rate estimate before opening all release points for the experiment. Calibrations were performed immediately prior to each

196 experiment to minimize pressure and temperature effects on orifice plate flow. Full details are provided by
197 Barchyn and Hugenholtz (2020a).
198



199
200 **Figure 5:** Overview of different pads at METEC and the facility. Each pad contains multiple equipment
201 units, typically grouped in like equipment. Pads 1 and 2 have one equipment group only. Figure after
202 Barchyn and Hugenholtz (2020a).
203

Pad	Equipment Group	Equipment Unit	
1	1 (wellhead, separator, tank)	1T-1 (tank)	
		1S-1 (separator)	
		1W-1 (wellhead)	
2	2 (wellhead, separator, tank)	2T-1 (tank)	
		2S-1 (separator)	
		2W-1 (wellhead)	
3	3W (wellheads)	3W-1 (wellhead)	
		3W-2 (wellhead)	
		3W-3 (wellhead)	
	3S (separators)	3S-1 (separator)	
		3S-2 (separator)	
	3T (tanks)	3T-1 (tank)	
		3T-2 (tank)	
	4	4W (wellheads)	4W-1 (wellhead)
			4W-2 (wellhead)
4W-3 (wellhead)			
4W-4 (wellhead)			
4W-5 (wellhead)			
4S (separators)		4S-1 (separator)	
		4S-2 (separator)	
		4S-3 (separator)	
		4S-4 (separator)	
4T (tanks)		4T-1 (tank)	
		4T-2 (tank)	
		4T-3 (tank)	
5		5W (wellheads)	5W-1 (wellhead)
	5W-2 (wellhead)		
	5W-3 (wellhead)		
	5S (separators)	5S-1 (separator)	
		5S-2 (separator)	
		5S-3 (separator)	
	4T (tanks)	4T-1 (tank)	
		4T-2 (tank)	
		4T-3 (tank)	

204

205 **Table 1:** *Equipment hierarchy and listing. Each experiment was conducted on a given pad. Results are*
206 *aggregated by equipment group and individual equipment units. Each equipment unit subsequently*
207 *contains multiple emissions points that are aggregated here. Note that Pad 5 included the tank complex*
208 *from Pad 4.*

209

210 Table 1 provides a full equipment listing used in this study (after Barchyn and Hugenholtz, 2020a). The
211 experiment pads used in this study differ in size and shape. Pads 1 and 2 were small and clustered, with
212 only 1 equipment group each. The tanks on Pads 1 and 2 were smaller (~100 - 200 barrel). Pads 3, 4, and 5
213 contained 3 different equipment groups each and had much larger tanks (~300 - 400 barrel).

214
215 The characteristics of pads at METEC were quite realistic. All pads had driving access around all sides of
216 all equipment groups. There was no road access in between individual pieces of equipment within a given
217 equipment group. This noted, there was no ground-level or overhead piping between equipment groups that
218 can reduce driving access on upstream oil and gas pads.

219 220 **4.2. Experimental protocol**

221 For each pad experiment, the METEC team created an emissions profile with 1-6 emissions points,
222 releasing methane at constant flow rates. Some pad configurations were replicates of previous pads. Pads
223 were tested in the order 1, 3, 5, 2, 4, then repeated. This protocol helped ensure the next pad was far from
224 the present pad and helped ensure that each pad had an equal number of experiments. In cases where the
225 upcoming pad was downwind of the target pad, calibrations were run without risk of interference.
226 Interference from any non-target methane releases was actively monitored.

227
228 The quantification tests were designed to emulate a standard measurement work practice with
229 approximately 3-4 downwind passes through the target plumes. Testing proceeded in all weather. We
230 qualify results with weather data. Wind speed and direction data were recorded from the PoMELO system.
231 No ancillary data were used or are reported.

232 233 **4.3. Analyses**

234 The goal of the analyses was to (i) evaluate the new quantification engine, (ii) understand the general bias
235 of the model to create an empirical correction, and (iii) evaluate the pattern of variance and effect of
236 controlling parameters on quantification results.

237
238 We first pre-processed the raw emissions data. Each experiment had 1-6 emissions points. In most cases
239 these emissions points were spread among equipment on the mock pad (see Table 1 for equipment and pad
240 listing). However, there were cases where there was more than one emissions point on a single piece of
241 equipment. In these cases, we combined the emissions rates of those sources to produce a sum rate at the
242 equipment scale. For these points, the position and heights of the emissions points were averaged so location
243 metadata were as representative as possible.

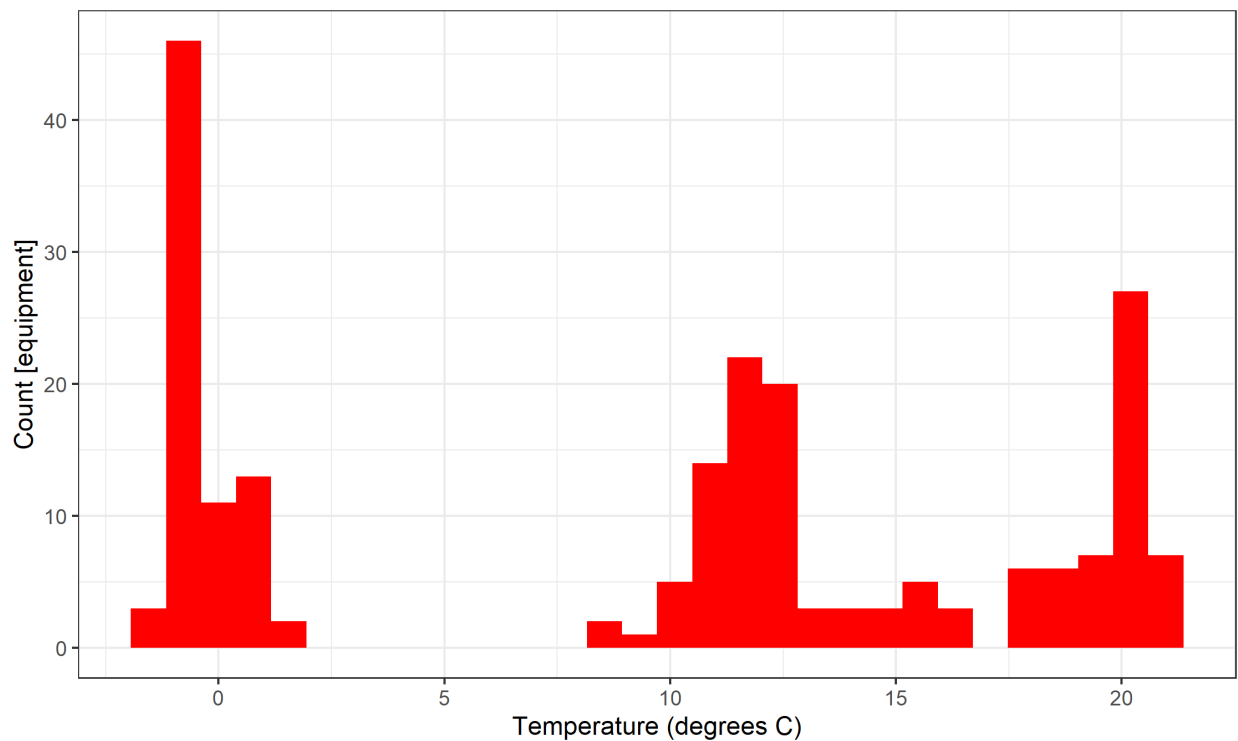
244
245 To produce emissions quantifications, we used the PoMELO quantification engine with the real emissions
246 point locations and measured PoMELO data from each pad. No additional data were used. The model
247 produces raw, theoretical emissions estimates. We compare these emissions estimates against the real
248 emissions rates to understand the fit and triage effectiveness as measured with proportion of explained
249 variance (r^2 of a linear model fit). We then use the linear model fit to determine a calibration factor for
250 subsequent residual analysis.

251
252 We elected to use all data in the dataset for testing and calibration as while this dataset is large ($n = 208$)
253 compared to similar studies (see Ravikumar et al., 2019; Johnson et al., 2021; Sherwin et al., 2021), it is
254 not large enough to split into test / train subsets without compromising the representativeness of test sets.
255 Future work may better evaluate the system efficacy in a different configuration.

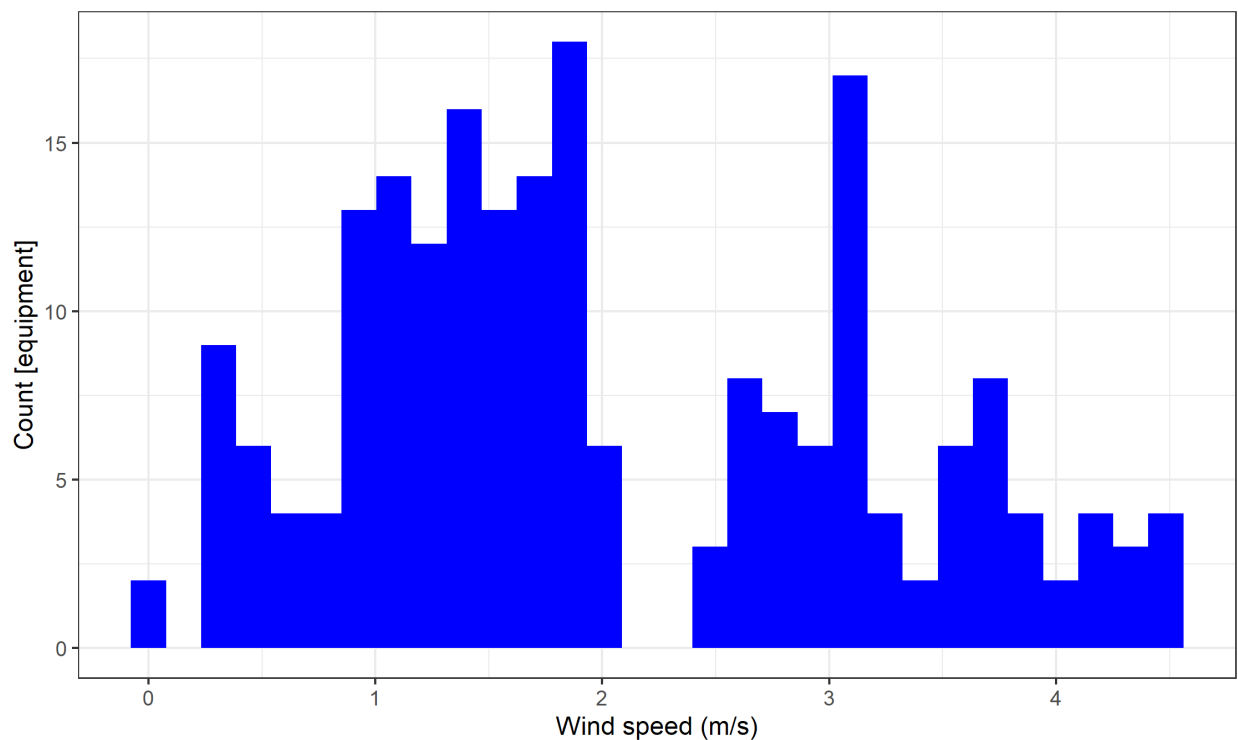
256 257 **5. Results and discussion**

258 **5.1. Experiment conditions**

259 Emissions quantification algorithms are often sensitive to environmental conditions (Fox et al., 2019a).
260 Performance assessments are better when they cover a wide range in conditions that more closely mimic
261 real deployment conditions.
262



263
264 **Figure 6:** Histogram of survey temperatures for each measured emissions point ($n = 209$).
265



267 **Figure 7: Distribution of survey wind speeds for each measured emissions point (n = 209).**
268

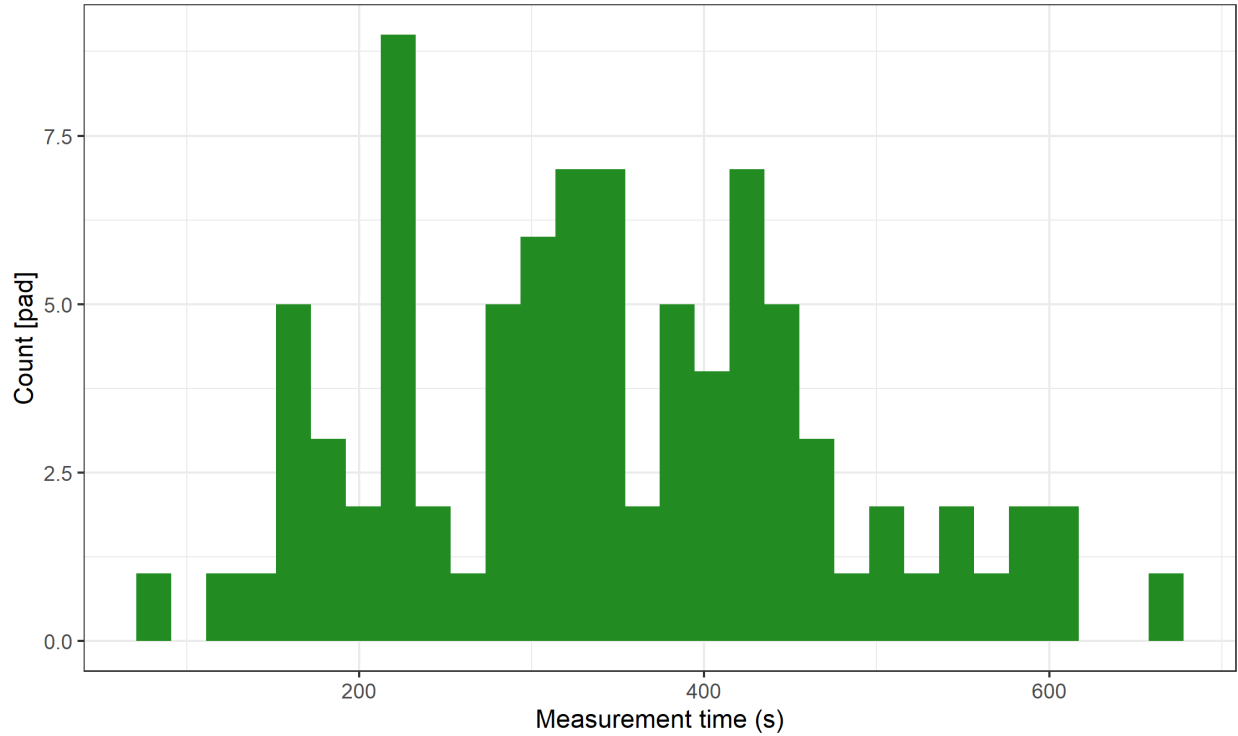
269 The test envelope was reasonably broad (Figures 6, 7). However, we were unable to test the system in
270 colder temperatures typical of Canadian winters (< -10 °C), extreme temperatures of Texas summers (> 35
271 °C), or in stronger winds (> 5 m/s). This noted, we were able to obtain a broad sample of atmospheric
272 conditions.

273
274 The atmospheric turbulence characteristics of the experiments are representative of prairie conditions.
275 Although METEC itself is an open field, the surrounding surface roughness and topography is diverse.
276 METEC is approximately 2 km E of the front range foothills of the Rocky Mountains which rise steeply.
277 To the S and E, the city of Fort Collins presents considerable surface roughness with reasonably flat
278 topography. To the N, a natural area represents a smooth surface roughness representative of many prairie
279 environments.

280
281 The equipment onsite affected airflow, but in a similar manner to real oil and gas infrastructure. Of note,
282 all equipment was open (similar to most infrastructure in the United States or other warm climates).
283 Separators were not in small, heated buildings, as is common in Canada or other colder climates. Tanks
284 were clustered, bermed, and varied in size as is common on upstream oil and gas sites. For the PoMELO
285 system, the presence of realistic airflow interference is important to metric the performance of the system
286 as measurements are typically taken < 10 m from the equipment. Airflow effects materially affect nearly
287 all plume models as eddies in the lee of large equipment confuse flow modeling algorithms.

288 289 **5.2. PoMELO survey characteristics**

290 The PoMELO system was driven in a normal survey manner for each experiment to emulate normal
291 operations, with > 3 laps of each equipment group (Figure 8 shows survey times). We drove all pads at a
292 normal driving pace for upstream pads in an effort to emulate real operations.
293

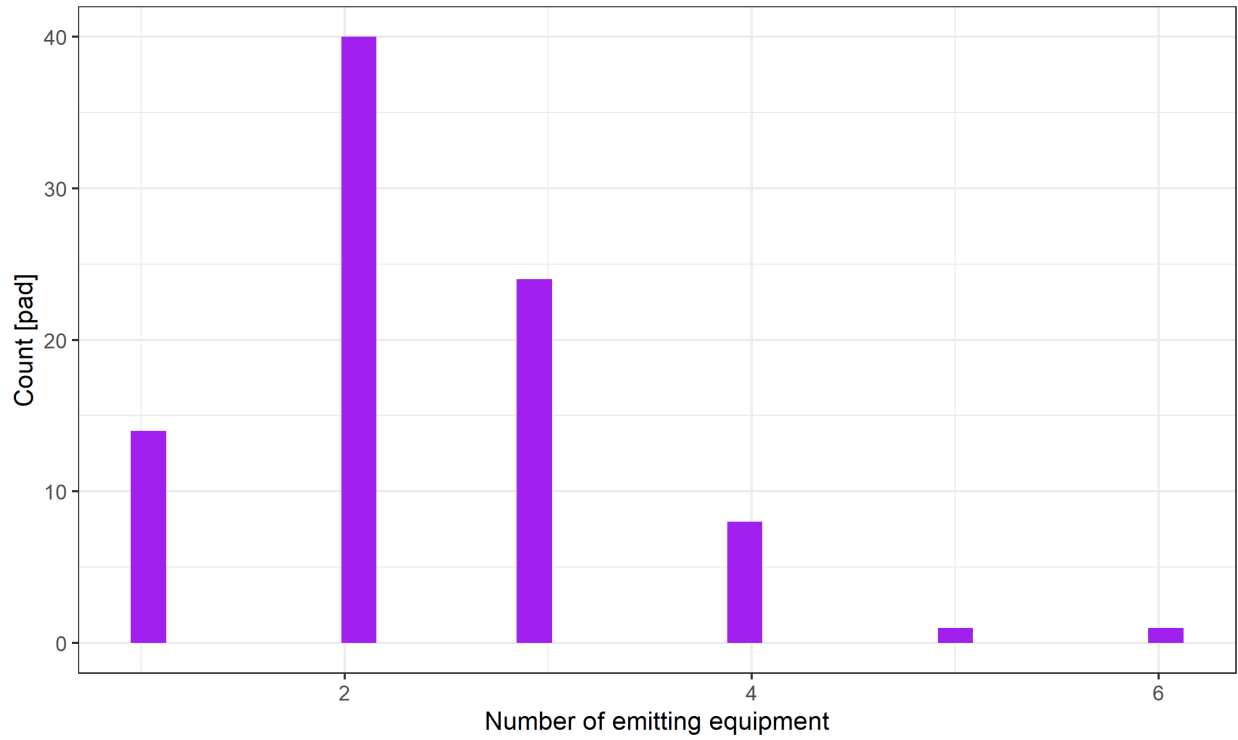


294 **Figure 8:** Survey time for each experiment. Note that survey time is recorded by the system and does not
 295 include time for reporting which is completed after turning off the system. Note that pads are not equal
 296 sized and longer survey times do generally correspond to the larger pads (Pad 3, 4, 5).
 297
 298

299 From theoretical consideration of close-range plume models, longer survey times are expected to increase
 300 accuracy and shorter survey times (< 200 s) are expected to reduce accuracy. As such, the survey times
 301 used here are important data to context all quantification results. This noted, the sites here are small and
 302 survey times should be expected to scale with site complexity and number of equipment present. For
 303 example, to achieve similar results in surveys of large gas plants, survey times will correspondingly need
 304 to scale.

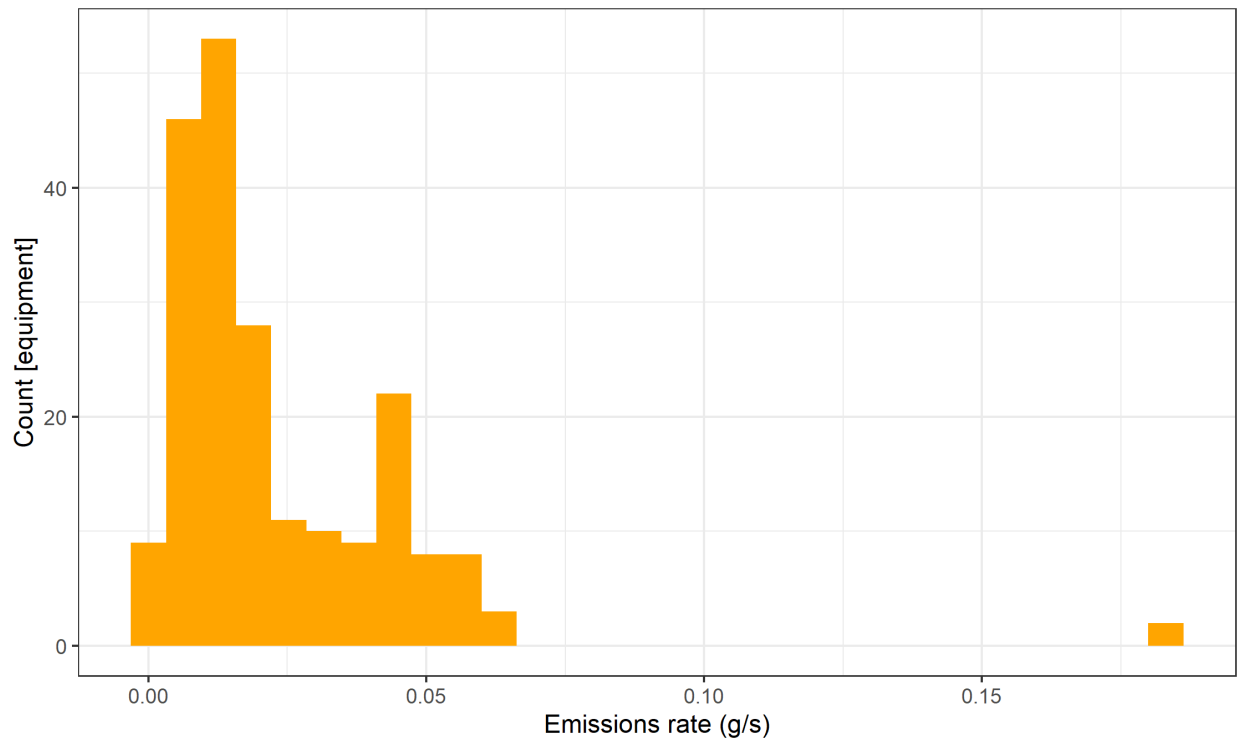
305 5.3. Pad characteristics

306 Prior to reporting measured results, we context the pad characteristics (Figures 9, 10). These characteristics
 307 were designed to emulate similar experiments (Ravikumar et al., 2019), but also were designed to explore
 308 the limitations of the PoMELO system. We did not conceptually or practically separate vents from leaks –
 309 typically this is performed at the follow-up stage with close range survey methods and is outside of the
 310 scope of these experiments (Barchyn and Hugenholtz, 2020a).
 311
 312



313
314
315
316

Figure 9: Number of emitting equipment per survey ($n = 88$). Equipment listings for each pad are presented in Table 1.



317
318
319

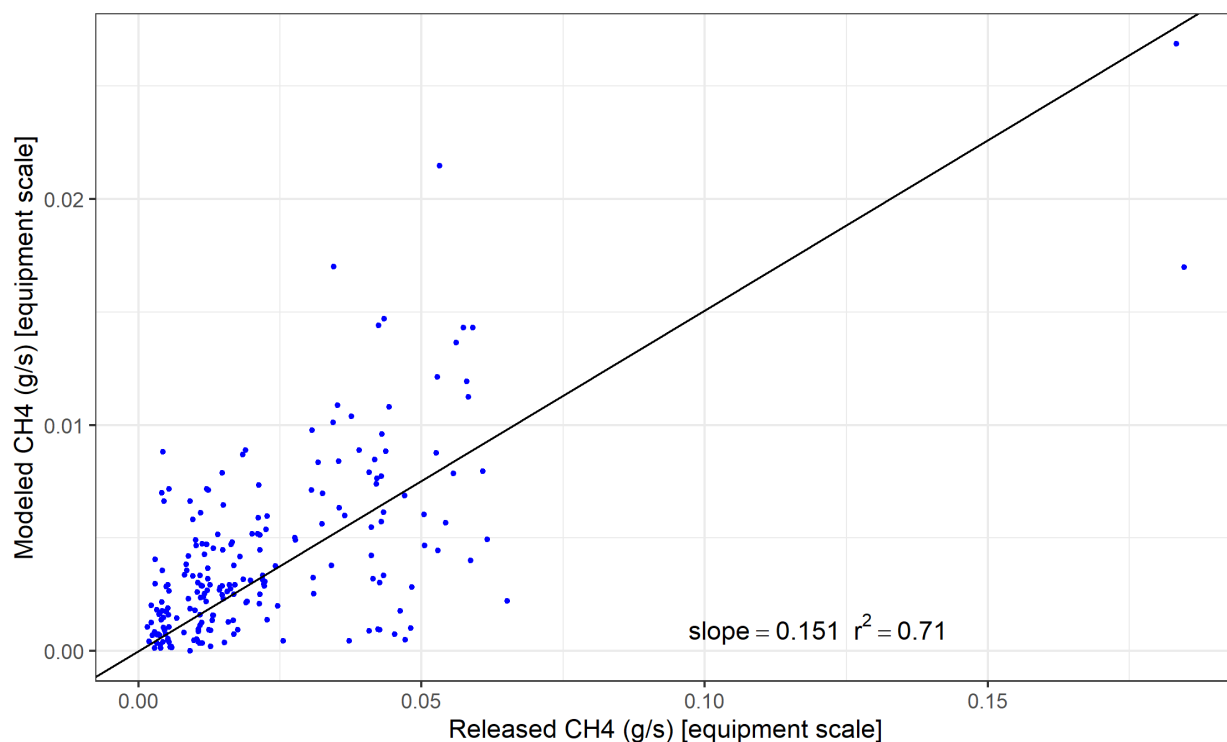
Figure 10: Sum of emissions rates for each equipment in g/s CH_4 ($n = 88$).

320 The equipment emissions rates are generally similar to those of Ravikumar et al. (2019). These rates are
321 much lower than empirically measured total pad emissions. For example, Zavala-Araiza et al. (2018)
322 reported average total pad emissions of 1.52 g/s in Alberta, Canada, measured empirically from off-site.
323 We used much lower rates as the PoMELO system is quite sensitive to small emissions rates and we sought
324 to benchmark the skill of the system at these lower rates. Additionally, METEC was not well equipped for
325 emitting large emissions rates.

326 327 **5.4. PoMELO quantification results**

328 To evaluate the PoMELO quantification engine, we first compared the raw uncalibrated results against the
329 real emissions rates. A simple least-squares linear model was fit to the data (see Figure 11) to evaluate the
330 proportion of explained variance and to create a calibration factor. The calibration factor from the simple
331 linear regression is 6.77 (slope = 1.151), with a fit $r^2 = 0.71$, $n = 208$.

332

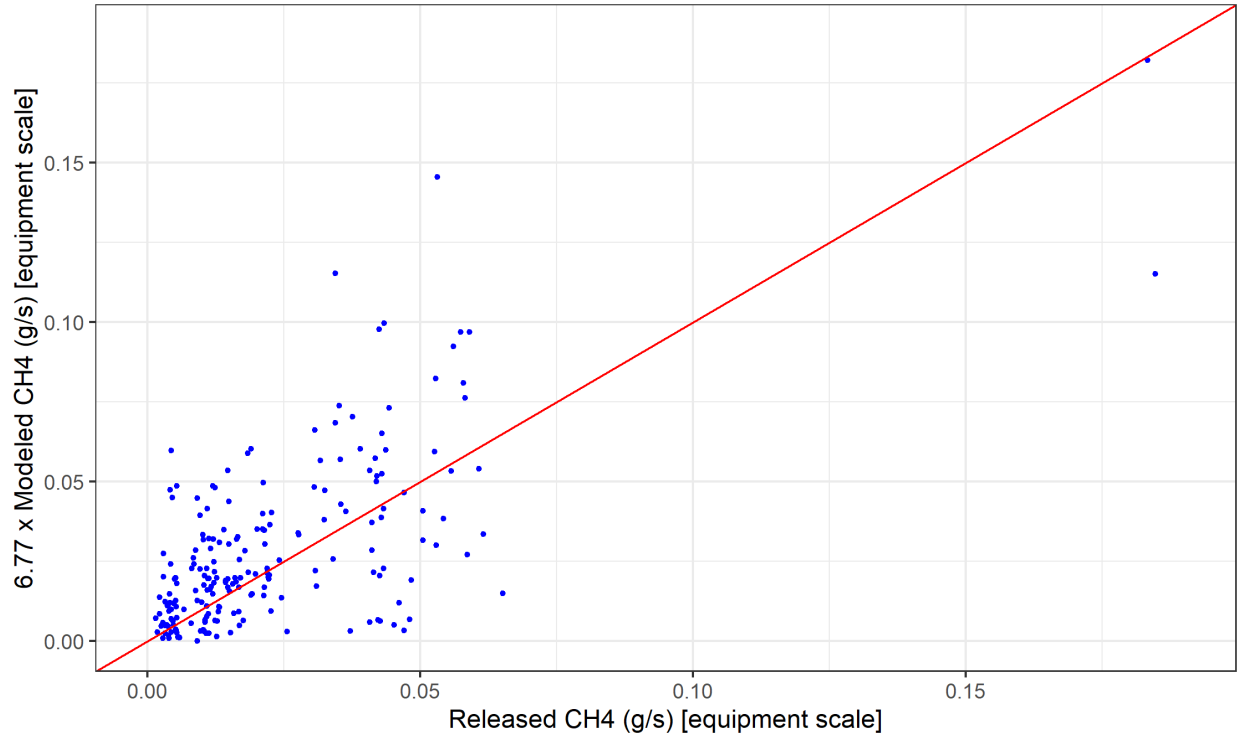


333
334 **Figure 11:** Uncalibrated model data against released rates on the equipment scale. See Figures 9 and 10
335 for equipment characteristics.

336
337 This suggests that the theoretical model underpredicts the real emissions rates by a factor of approximately
338 6.77. This is expected, the theory of the model systematically underpredicts emissions rates and requires
339 calibration to produce meaningful emissions rates.

340
341 This dataset is the largest controlled release dataset among similar technologies to the authors knowledge
342 (see similar studies from Ravikumar et al., 2019; Sherwin et al., 2021; Singh et al., 2021). Due to the size
343 and representativeness of this dataset, this calibration factor should be relatively robust, but further tests
344 could help better calibrate the model in the future. The proportion of explained variance ($r^2 = 0.71$) suggests
345 that the model is capturing a reasonable proportion of the variance associated with emissions releases.

346



347
 348 **Figure 12:** Calibrated model results (raw model results multiplied by empirical calibration of 6.77) against
 349 released rates. Red line has a slope of 1.0, intercept of 0.0, provided for reference.

350
 351 **5.5. Condition dependence**

352 Evaluating condition dependence is vital for plume models for several reasons: (i) valuable information on
 353 where the theoretical model is failing can be explored, helping improve future versions of the model, and
 354 (ii) condition dependence provides important practical information on environmental conditions where poor
 355 quantification performance can be expected, helping PoMELO operators take this into account when
 356 working on pads.

357
 358 We used scaled residuals to metric the performance of the model following
 359

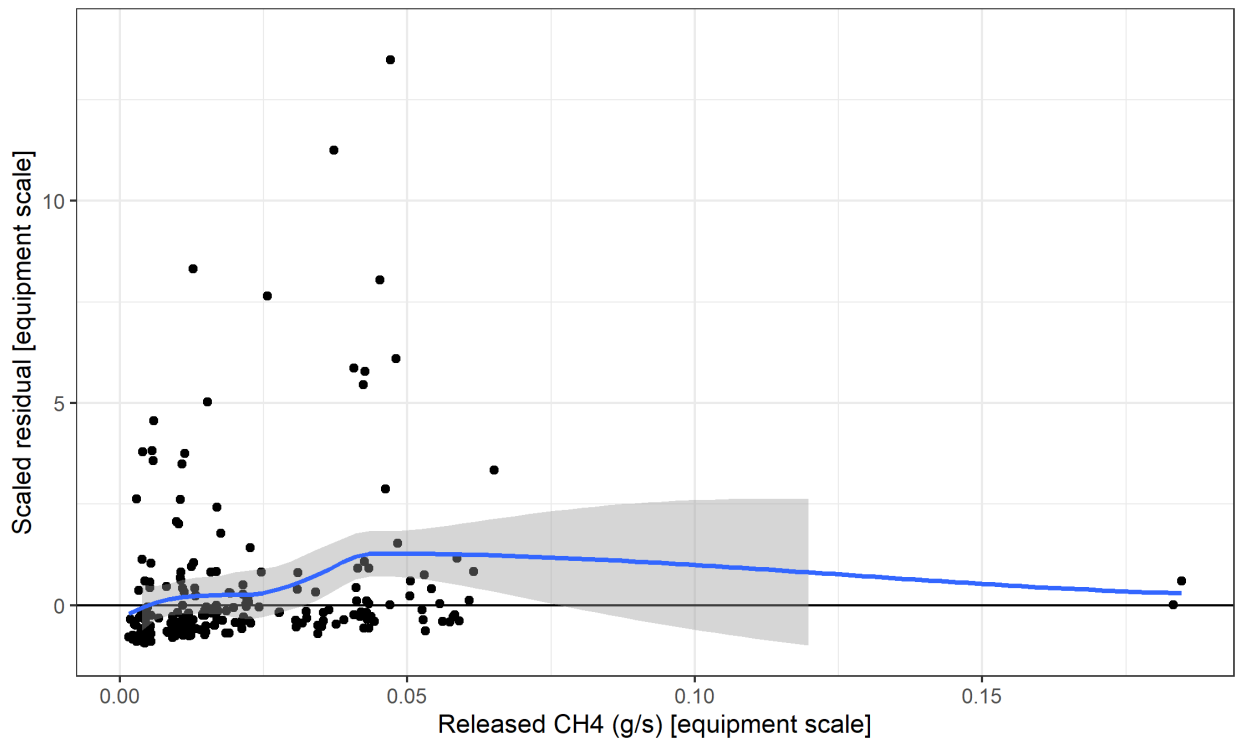
360
$$\text{Scaled residual} = \frac{Q_{\text{released}} - 6.77 \cdot Q_{\text{estimated}}}{6.77 \cdot Q_{\text{estimated}}} \quad (1)$$

361
 362 where Q_{released} is the released emissions rate in g/s methane, $Q_{\text{estimated}}$ is the estimated emissions rate in g/s
 363 methane. The 6.77 multiplied by estimated rates is the empirical calibration factor determined above. Our
 364 scaled residual has the properties where:

- 365
 366
 - -1.0 corresponds to situations where the model substantially overpredicted the emissions rate.
 - 0.0 corresponds to situations where the model perfectly predicted the emissions rate.
 - >1.0 corresponds to situations where the model substantially underpredicted the emissions rate.

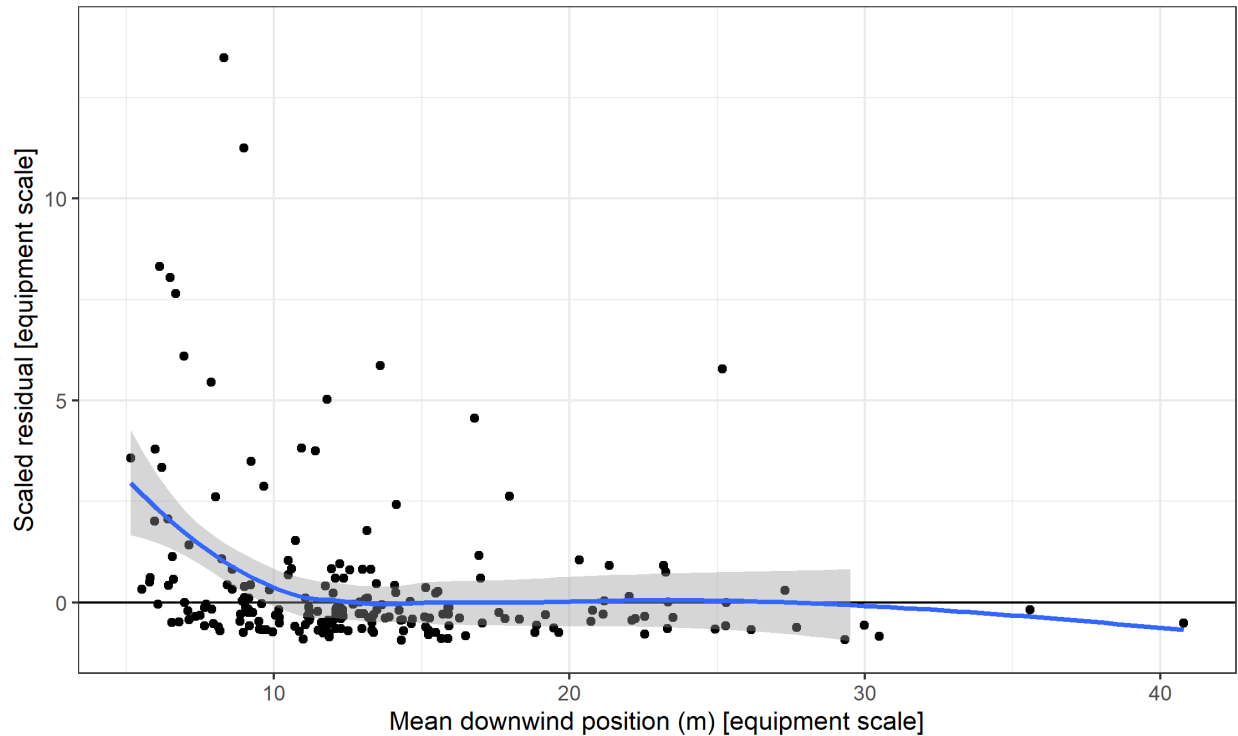
369
 370 The purpose of scaling the residual against estimated emissions rates is to consider the performance
 371 normalized to measured concentration, which scales approximately linearly to estimated emissions rate.
 372 The range of enhancements measured here are well resolved with the methane sensor, thus a large

373 proportion of the error in the plume model can be sourced directly to the plume model itself, independent
374 of emissions rate.
375



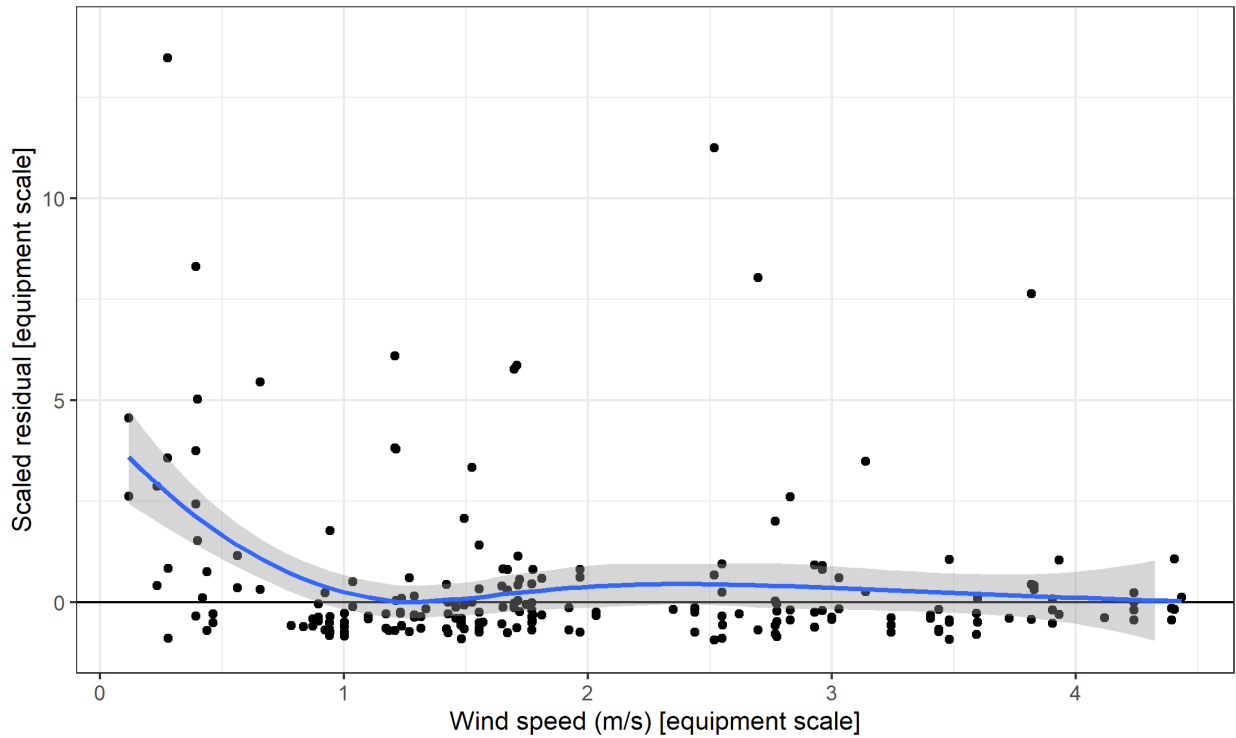
376
377
378 **Figure 13:** Scaled residuals against release rates. A simple loess fit is shown to help highlight any trends.
379 Note: one data point is omitted from this plot to improve interpretability (scaled residual = 857.9).

380
381 Comparing the scaled residuals against release rates (Figure 13) does not reveal considerable trends but
382 does emphasize the skew of release rates to small emissions rates and variable data density. The lack of
383 clear trend is expected from theory and from the calibration. The model should not be significantly affected
384 by release rate as most measured concentrations are well above the inherent noise of the concentration
385 measurements from the methane sensor, and the dominant source of error is related to the behaviour of the
386 plume.
387

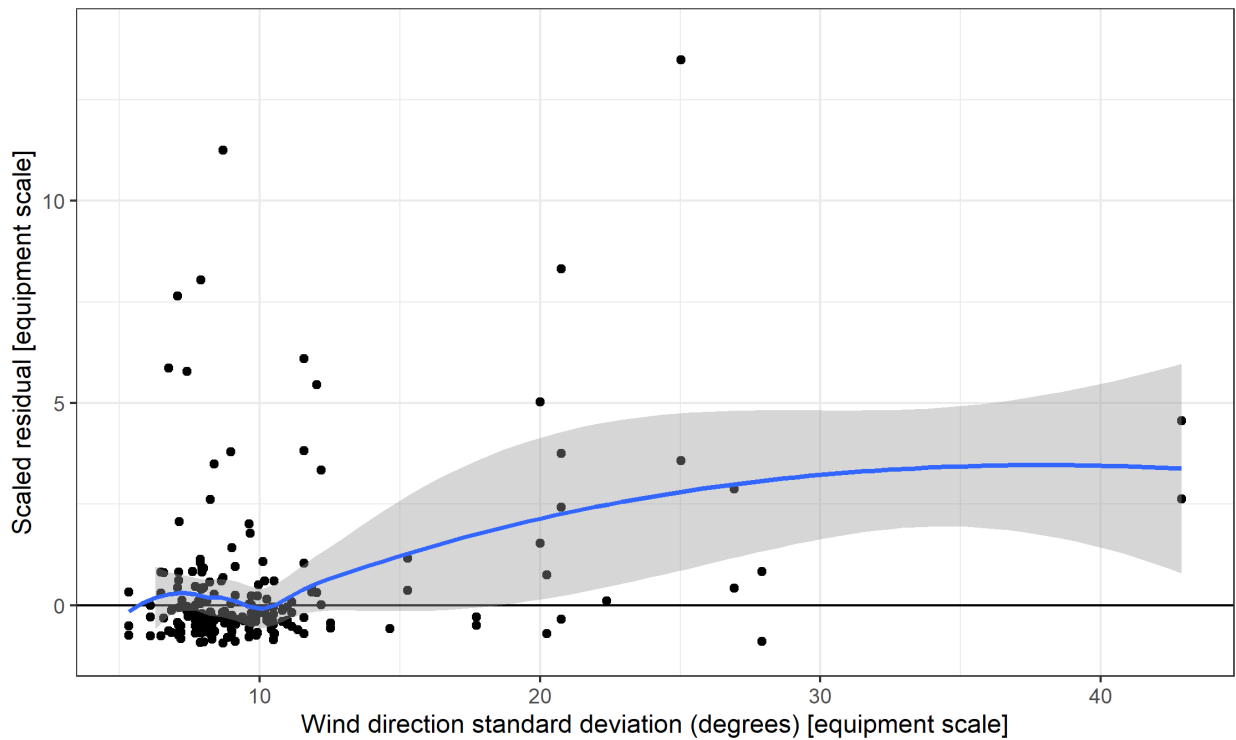


388
 389 **Figure 14:** Scaled residuals against mean downwind measurement position. A simple loess fit is shown to
 390 help highlight any trends. Note: one data point is omitted from this plot to improve interpretability (scaled
 391 residual = 857.9).
 392

393 Figure 14 shows the mean downwind position of the most important concentration measurements used in
 394 the plume model. Large downwind positions indicate the plumes were dominantly measured from further
 395 downwind, smaller positions relate to situations where equipment was only measured at a very close range.
 396 Most of the significant underpredictions occurred where measurements were < 15 m from the release
 397 source. This is somewhat expectable as plume behaviour at very close ranges is dominated by small scale
 398 turbulence in the lee of equipment. This is important and helps to justify the experimental setup at METEC,
 399 which uses real equipment similar to upstream sites. The airflow effects of the equipment at METEC are
 400 likely partially responsible for the increase in error seen in Figure 14. It is possible this effect may not be
 401 observed in controlled releases with isolated release stacks that do not significantly affect airflow (e.g.,
 402 Johnson et al., 2021; Sherwin et al., 2021; Singh et al., 2021).
 403



404
 405 **Figure 15:** Scaled residuals against wind speed. A simple loess fit is shown to help highlight any trends.
 406 Note: one data point is omitted from this plot to improve interpretability (scaled residual = 857.9).
 407

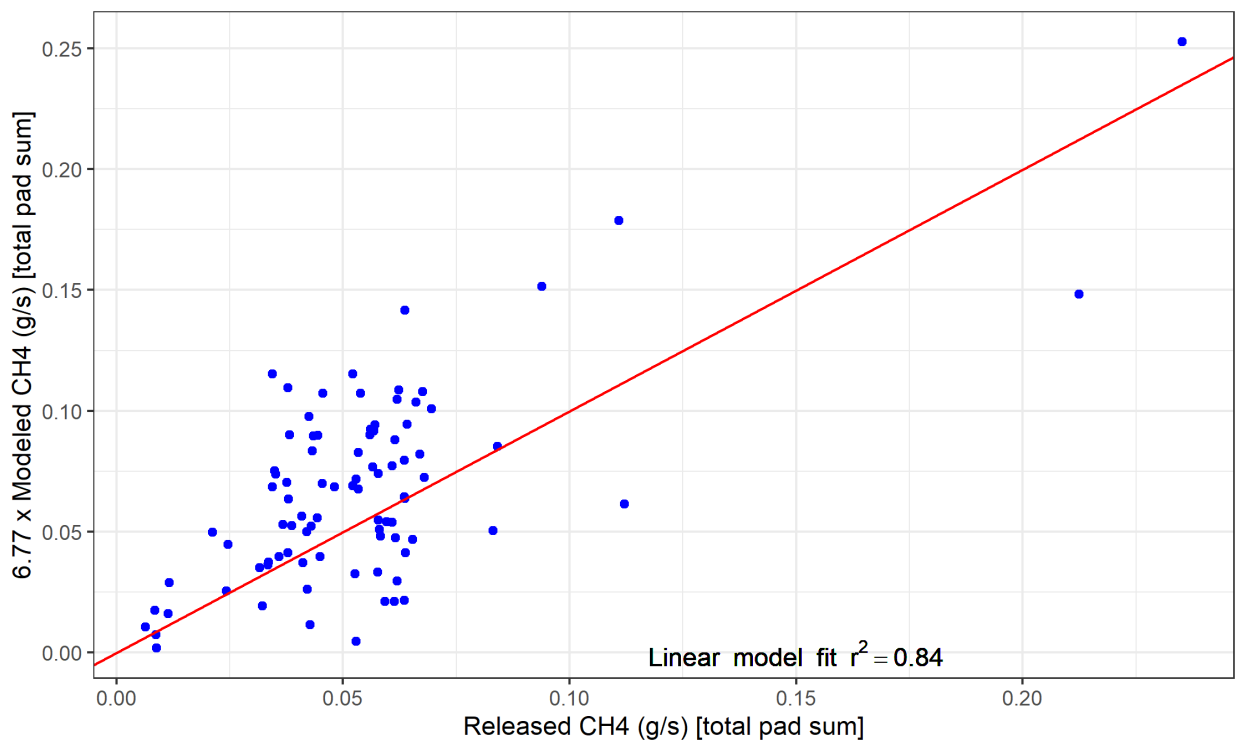


408
 409 **Figure 16:** Scaled residuals against wind direction standard deviation. A simple loess fit is shown to help
 410 highlight any trends. Note: one data point is omitted from this plot to improve interpretability (scaled
 411 residual = 857.9).

412
413 Figures 15 and 16 show wind speed and direction variability metrics against error. Conditions with very
414 low wind speeds (< 1 m/s) and high wind direction variability (> 15 degrees) relate with underpredictions
415 and a large increase in error. From theory, this is expectable; plumes are significantly more difficult to
416 model in conditions where the advection of air from source to sensor is less certain. The model does appear
417 to be robust in conditions with consistent wind (> 1 m/s) across a range of wind speeds with little wind
418 speed dependence.

419
420 **5.6. Combined pad results**

421 The PoMELO quantification engine is designed to de-mix contributions from multiple sources in close
422 proximity. Many pads contained sources in very close proximity where plumes were mixed (Figure 5). This
423 is a particularly complex and error-prone part of the plume model. In situations where there are multiple
424 close emissions points, it is likely that while individual emissions rates for the contributing sources may
425 have higher error, the sum of all emissions rates may be accurate.
426



427
428 **Figure 17:** Pad sum calibrated emissions rates against released emissions rates. The red line is a 1:1 line
429 for reference ($n = 88$).

430
431 Figure 17 shows the sum of all emissions sources on each pad compared to the calibrated estimated sum of
432 all sources. As expected, there is better fit, with a proportion of linear model explained variance (r^2)
433 increasing to 0.84 (from 0.71 when considering each equipment emissions separately).

434
435 This suggests that the model can produce more accurate results for total pad emissions estimations when
436 summing the constituent emissions points at the equipment scale. This has relevance for practical
437 application in jurisdictions where a total site rate is of interest.
438

439 **5.7. Comparison with other technologies**

440 The PoMELO system is designed for on-pad measurements of equipment-scale emissions rates. Here we
 441 compare the proportion of explained variance of different systems with previously published controlled
 442 release data.

443

Technology	Experiment characteristics	Prop. of explained variance (linear model r^2)	n	Reference	Notes
PoMELO	mixed plume	0.71	209	This study	Totals of all equipment on a site improve on these results ($r^2 = 0.84$, see Figure 17)
Heath Consultants Inc.	mixed plume	0.44	23	Ravikumar et al. (2019)	
Seek Ops Inc.	mixed plume	0.42	63	Ravikumar et al. (2019)	
Aeris Technologies	mixed plume	0.25	N/A	Ravikumar et al. (2019)	
Ball Aerospace	mixed plume	0.23	32	Ravikumar et al. (2019)	
Advisian	mixed plume	0.13	33	Ravikumar et al. (2019)	
Baker Hughes (GE)	mixed plume	0.10	57	Ravikumar et al. (2019)	
Picarro	mixed plume	0.04	86	Ravikumar et al. (2019)	
ABB / ULC Robotics	mixed plume	0.01	28	Ravikumar et al. (2019)	
Bridger Photonics Gas Mapping LiDAR™	single plume	0.87-0.89	N/A	Bridger Photonics (2021)	Results vary with choice of modeled wind.
Kairos Aerospace	single plume	0.67-0.84	173	Sherwin et al. (2021)	Results vary with choice of modeled wind. Slightly better results can be obtained with ground anemometers (see Sherwin et al., 2021)
Providence Photonics QL-320 QOGI	single plume	0.60	N/A	Singh et al. (2021)	
Altus Geomatics (now Geo Verra)	single plume	0.05	N/A	Singh et al. (2021)	

444
 445 **Table 2:** Comparison of equipment scale controlled release results for similar mobile emissions
 446 measurement technologies. Refer to references for full experimental context. Experiments with single
 447 plumes are separated from experiments with mixed plumes and closely situated equipment. Johnson et al.
 448 (2021) performed a blind assessment of Bridger Photonics Gas Mapping LiDAR™, but we excluded these
 449 results due to the small sample size of 11. Note that these results are only valid at the time of experiment,
 450 technology providers may have changed algorithms or technology.
 451

452 Table 2 suggests that PoMELO compares favourably, and particularly so in the more realistic multi-source
453 mixed plume configuration. We may conduct future experiments with single plume configurations, but
454 these configurations are often not representative of upstream pads.
455

456 **5.8. Expected sources of error and discussion of error reducibility**

457 The PoMELO system produces quantifications with several minutes of truck collected data. This approach
458 has a number of advantages and disadvantages with respect to expected sources of error. We discuss these
459 sources of error and general potential for future error reducibility. From first principles, emissions
460 quantification nominally relies upon accurate measurement of (i) the situation (sources, receptors, etc.), (ii)
461 the wind speed, and (iii) the methane concentration.
462

463 The situational measurements in PoMELO are quite accurate as the vehicle is physically on the site and
464 uses high quality location information from the GNSS (nominally < 1.2 m 1 standard deviation, depending
465 on satellite view and correction service availability, normally < 0.3 m). Most situational errors in PoMELO
466 surveys come from positioning the sources. In this study we include the real emissions point locations from
467 METEC. While the system as deployed includes a number of built-in user interface aids and systems to
468 locate emissions points as accurate as possible, picking the actual emissions point location requires care,
469 and it is likely that error will be introduced from equipment positioning during real deployments. Other
470 technologies face similar barriers and likely have similar sensitivities (Bridger Photonics, 2021; Sherwin et
471 al., 2021; Singh et al., 2021).
472

473 Situational complexity has a large and expectable impact on quantification accuracy when considering
474 mixed plumes (Figure 1). As shown in Figures 17 and 12, results improve when considering the sum of
475 emissions points on a given pad. This is expectable as de-mixing the relative contributions of several close
476 sources is difficult and error prone. METEC has the advantage of including relatively realistic equipment
477 configurations with closely spaced equipment. Sherwin et al. (2021) describe how the Kairos Aerospace
478 aircraft system they tested could not disambiguate plumes from multiple release points 15 m apart,
479 suggesting that ground-based systems have advantages for practical emissions point measurement on
480 upstream pads with closely situated equipment.
481

482 Methane concentration measurements are generally quite accurate with the PoMELO system because in-
483 situ laser spectrometers are a very mature and a well-understood mode of instrumentation. The largest
484 source of error for ground-based methods is not the instrumentation itself, but rather the ability to generalize
485 the shape of the plume and understand the portions of the plume that are above the vehicle. This is likely
486 manifest in the defined decrease in quantification accuracy for sources measured close to the vehicle (Figure
487 14). Airborne systems, in general, have a much higher minimum detection limit than PoMELO (Johnson et
488 al., 2021; Sherwin et al., 2021), which suggests that airborne methods have more noise in measurements of
489 concentration than vehicle systems. This noted, airborne systems can fully resolve the vertical distribution
490 of the plume, which can translate to a more complete portrait of plumes.
491

492 Recent studies such as Cusworth et al. (2022) have found a considerable large number of large emissions
493 sources across U.S. oil and gas production. The emissions rates released in this study were very small
494 compared to the ‘super-emitters’ or ‘ultra-emitters’ documented by these high-profile missions. It is helpful
495 to consider whether PoMELO could feasibly measure these large emissions sources from first principles.
496 In the case of unlit flares, PoMELO would likely be unable to produce accurate quantifications while on
497 pads as the release points are normally too high and don’t advect to the surface. This could reduce the
498 efficacy of PoMELO for quantifying emissions from unlit flares; however, from the perspective of detecting

499 and rectifying the issue, unlit flares can normally be visibly seen and investigated while on site, without the
500 use of any technology. For other large emissions points, this depends on the concentration in the air. The
501 methane sensor on PoMELO ranges out at approximately 70 ppmv and ceases to produce accurate data.

502
503 The structure of most plume models (PoMELO included) linearly relates concentration to emissions rate,
504 so as long as the concentration does not exceed the measurement capacity of the sensor, the same accuracy
505 of results can be expected. In situations where the methane sensor is ranging out – it is immediately clear
506 to the PoMELO operator that serious quantities of hydrocarbons are in the atmosphere on the site. Thus, in
507 many practical situations, this instrument response may be sufficient to trigger action.

508
509 Emissions flux is generally concentration multiplied by wind speed (mass x advection) – thus the ability
510 for a given technology to resolve wind speed has important effect on quantification accuracy and in
511 situations dominates the error budget. PoMELO uses high resolution mobile anemometry to resolve the
512 flow field on the site at 10 Hz and considers the spatial configuration of flow measurements. Wind
513 measurements from PoMELO are quite accurate in a relative sense, but there are errors associated with
514 mobile anemometry – some of which are likely causing issues with quantification in extremely low wind
515 speed situations (see Figure 15 and 16).

516
517 However, it is important to note that PoMELO *measures* wind on the site at the exact time when
518 concentration measurements are collected. This contrasts with aircraft-based systems, which suffer from
519 well documented errors associated with estimating ground wind speed (Johnson et al., 2021; Sherwin et al.,
520 2021). For most aircraft deployments, ground wind speed is usually estimated from modeled wind forecast
521 products. While these products can be accurate in regions with flat topography, well-established boundary
522 layer flow, homogenous land cover, and proximity to weather stations (that feed into the wind modeling
523 systems) - in many more remote regions or locations with topography errors are large (Johnson et al., 2021).
524 Sherwin et al. (2021) demonstrate that different averaging and data extraction schemes for wind data from
525 the US NOAA HRRR wind model could materially affect results, with r^2 fits ranging from 0.39 to 0.67 (see
526 Figure S17, Sherwin et al., 2021). Further, the timescales of plume measurement for aircraft-based systems
527 are on the order of seconds – well within the timescales associated with boundary layer turbulence. Error
528 may be fundamentally irreducible with this approach – it is unlikely that any forecast wind model would
529 ever be able to accurately predict boundary layer turbulence.

530 531 **6. Conclusions**

532 This study outlines quantification performance of the University of Calgary PoMELO vehicle-based
533 measurement system. We tested the system against 209 individually metered emissions points at the CSU
534 METEC facility. In particular, we tested situations with complex mixed plumes, similar to real upstream
535 oil and gas production sites.

536
537 Results suggest the system can accurately triage individual emissions points ($r^2 = 0.71$), providing valuable
538 information on emissions rates. Results improved when considering the sum of all emissions points on each
539 pad ($r^2 = 0.84$). Conditions with stable, well-defined flow improved quantification performance. Similarly,
540 situations where measurements were very close to equipment were generally less accurate than those further
541 downwind.

542
543 Together, these results suggest the PoMELO system is likely to have practical utility for understanding and
544 managing emissions from individual equipment on upstream pads, providing important clarity for oil and
545 gas operators as they manage methane emissions.

546
547
548
549
550
551
552
553
554
555
556
557
558
559
560
561
562
563
564
565
566
567
568
569
570
571
572
573
574
575
576
577
578
579
580
581
582
583
584
585
586
587
588
589
590
591
592

7. References

- Alvarez, R.A., Zavala-Araiza, D., Lyon, D.R., Allen, D.T., Barkley, Z.R., Brandt, A.R., Davis, K.J., Herndon, S.C., Jacob, D.J., Karion, A., Kort, E.A., Lamb, B.K., Lauvaux, T., Maasackers, J.D., Marchese, A.J., Omara, M., Pacala, S.W., Peischl, J., Robinson, A.L., Shepson, P.B., Sweeney, C., Townsend-Small, A., Wofsy, S.C., Hamburg, S.P., 2018. Assessment of methane emissions from the U.S. oil and gas supply chain. *Science* 361, 186-188. DOI: 10.1126/science.aar7204.
- Barchyn TE, Hugenholtz CH, 2020a. University of Calgary Rapid Vehicle-based Methane Emissions Mapping System (PoMELO) Single-Blind Testing Results from the Methane Emissions Technology Evaluation Center (METEC). *Harvard Dataverse*. DOI: 10.7910/DVN/BUT8GA.
- Barchyn, T.E., Hugenholtz, C.H., 2020b. PoMELO METEC 2019 Data. Supporting data. *Harvard Dataverse*. DOI: 10.7910/DVN/7ZZKC7.
- Barchyn, T.E., Hugenholtz, C.H., Fox, T.A., 2019. Plume detection modeling of a drone-based natural gas leak detection system. *Elementa: Science of the Anthropocene* 7, 41. DOI: 10.1525/elementa.379.
- Bridger Photonics. 2021. Performance of Gas Mapping LiDAR™ for quantification of very high methane emissions rates. Bridger Photonics White Paper #210607. Available from: https://www.bridgerphotonics.com/sites/default/files/inline-files/BridgerPhotonics_HighControlledReleaseRates.pdf (accessed 14 March 2022).
- Cusworth, D.H., Thorpe, A.K., Ayasse, A.K., Stepp, D., Heckler, J., Asner, G.P., Miller, C.E., Chapman, J.W., Eastwood, M.L., Green, R.O., Hmiel, B., Lyon, D., and R.M. Duren. 2022. Strong methane point sources contribute a disproportionate fraction of total emissions across multiple basins in the U.S. *EarthArXiv*. DOI: 10.31223/X53P88.
- Fox, T.A., Barchyn, T.E., Risk, D., Ravikumar, A.P., Hugenholtz, C.H., 2019a. A review of close-range and screening technologies for mitigating fugitive methane emissions in upstream oil and gas. *Environmental Research Letters* 14, 053002. DOI: 10.1088/1748-9326/ab0cc3.
- Fox, T.A., Ravikumar, A.P., Hugenholtz, C.H., Zimmerle, D., Barchyn, T.E., Johnson, M.R., Lyon, D., Taylor, T., 2019b. A methane emissions reduction equivalence framework for alternative leak detection and repair programs. *Elementa: Science of the Anthropocene* 7, 30. DOI: 10.1525/elementa.369.
- Fox, T.A., Hugenholtz, C.H., Barchyn, T.E., Gough, T.R., Gao, M., Staples, M., 2021. Can new mobile technologies enable fugitive methane reductions from the oil and gas industry? *Environmental Research Letters* 16, 064077. DOI: 10.1088/1748-9326/ac0565.
- Johnson, D., Heltzel, R., and D. Oliver. 2019. Temporal variations in methane emissions from an unconventional well site. *ACS Omega* 4, 3708-3715. DOI: 10.1021/acsomega.8b03246.
- Johnson, M.R., Tyner, D.R., and A.J. Szekeres. 2021. Blinded evaluation of airborne methane source detection using Bridger Photonics LiDAR. *Remote Sensing of Environment* 259, 112418. DOI: 10.1016/j.rse.2021.112418.

- 593 Ocko, I.B., Sun, T., Shindell, D., Oppenheimer, M., Hristov, A.N., Pacala, S.W., Mauzerall, D.L., Xu, Y.,
594 and S.P. Hamburg. 2021. Acting rapidly to deploy readily available methane mitigation measures by
595 sector can immediately slow global warming. *Environmental Research Letters* 16, 054042. DOI:
596 10.1088/1748-9326/abf9c8.
- 597
- 598 Ravikumar, A.P., Sreedhara, S., Wang, J., Englander, J., Roda-Stuart, D., Bell, C., Zimmerle, D., Lyon,
599 D., Mogstad, I., Ratner, B., Brandt, A.R., 2019. Single-blind inter-comparison of methane detection
600 technologies – results from the Stanford/EDF Mobile Monitoring Challenge. *Elementa: Science of the*
601 *Anthropocene* 7, 37. DOI: 10.1525/elementa.373.
- 602
- 603 Sherwin, E.D., Chen, Y., Ravikumar, A.P., and A.R. Brandt. 2021. Single-blind test of airplane-based
604 hyperspectral methane detection via controlled releases. *Elementa: Science of the Anthropocene* 9,
605 00063. DOI: 10.1525/elementa.2021.00063.
- 606
- 607 Singh, D., Barlow, B., Hugenholtz, C.H., Funk, W., Robinson, C., and A.P. Ravikumar. 2021. Field
608 performance of new methane detection technologies: Results from the Alberta Methane Field
609 Challenge. *EarthArXiv*. 10.31223/X5GS46.
- 610
- 611 Zavala-Araiza, D., Herndon, S.C., Roscioli, J.R., Yacovitch, T.I., Johnson, M.R., Tyner, D.R., Omara,
612 M., Knighton, B., 2018. Methane emissions from oil and gas production sites in Alberta, Canada.
613 *Elementa: Science of the Anthropocene* 6, 27. DOI: 10.1525/elementa.284.
- 614
- 615 Zimmerle, D., Vaughn, T., Bell, C., Bennett, K., Deshmukh, P., Thoma, E., 2020. Detection limits of
616 optical gas imaging for natural gas leak detection in realistic controlled conditions. *Environmental*
617 *Science and Technology* 54, 11506-11514. 10.1021/acs.est.0c01285.
- 618
- 619 Zimmerle, D., Duggan, G., Vaughn, T., Bell, C., Lute, C., Bennett, K., Kimura, Y., Cardoso-Saldana,
620 F.J., Allen, D.T., 2022. Modeling air emissions from complex facilities at detailed temporal and spatial
621 resolution: the Methane Emission Estimation Tool (MEET). *Science of the Total Environment*, IN
622 PRESS. 10.1016/j.scitotenv.2022.153653.
- 623

624 **Acknowledgements**

625 We gratefully thank Clay Bell and Aidan Duggan at METEC for expert guidance, running of experiments,
626 and edits on previous version of this manuscript.

627